

A maze of solid solutions of pimobendan enantiomers: an extraordinary case of polymorph and solvate diversity

Toms Rekis*, Agris Bērziņš, Inese Sarceviča, Artis Kons, Mārtiņš Balodis, Liāna Orola, Heike Lorenz, and Andris Actiņš

* toms.rekis@lu.lv

1. Crystal forms of racemic pimobendan	1
1.1. Transitions of racemic pimobendan crystal forms.....	1
1.2. Polymorphs of racemic pimobendan	3
1.3. Hydrates of racemic pimobendan.....	3
1.4. Solvates of racemic pimobendan.....	4
2. DSC and PXRD data used to establish the melt phase diagram of pimobendan enantiomers.....	7
2.1. Solid solutions α and ζ	7
2.2. Solid solutions δ and γ	8
3. Evidence of solvated solid solutions of pimobendan enantiomer phases.....	11
4. Experimental and calculated PXRD patterns of <i>enant</i> -F	14

1. Crystal forms of racemic pimobendan

1.1. Transitions of racemic pimobendan crystal forms

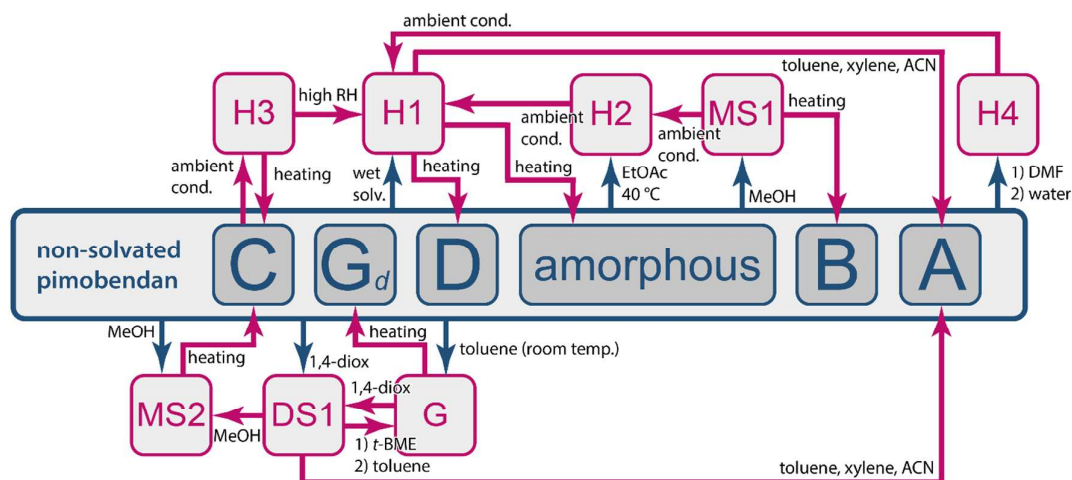


Figure S1. Principal transitions between the crystalline forms of racemic pimobendan showing the transition conditions.

Racemic pimobendan hydrate *rac*-H1 can be obtained by crystallization of pimobendan from organic solvents containing trace amount of water, by stirring a suspension of pimobendan and water, and by stirring a suspension of pimobendan in solvents containing trace amounts of water or absorbing water during the stirring from the air. By heating pimobendan hydrate *rac*-H1 at a high temperature (one hour at 140 – 150 °C or one week at 80 °C above P₂O₅), it transforms to anhydrous amorphous form. If amorphous form or hydrate *rac*-H1 is heated at more than 150 °C for longer than one hour, a polymorphic form appears, namely, *rac*-D.

When amorphous pimobendan or any pimobendan polymorph is suspended in methanol at low relative humidity (<5%) and the methanol is evaporated, methanol solvate *rac*-MS1 is obtained. Solvate *rac*-MS1 can also be prepared by storing any of pimobendan anhydrous forms or hydrate *rac*-H1 in a desiccator with methanol. If pimobendan is suspended in boiling methanol, mainly methanol solvate *rac*-MS1 forms, however, hydrate *rac*-H1 or even some other crystalline forms of pimobendan are usually present. When methanol solvate *rac*-MS1 is kept at 100 °C for one hour or stored at relative humidity lower than 3% at ambient temperature for 2 days, an anhydrous polymorphic form *rac*-B forms. If methanol solvate *rac*-MS1 is stored at relative humidity higher than 10% at ambient temperature, a new hydrate *rac*-H2 forms. *rac*-H2 can also appear when a small amount of solvent is added to any anhydrous form and suspension is evaporated in ambient conditions if relative humidity is below 30%, but in this case *rac*-H2 mainly forms together with other crystalline phases.

When pimobendan is crystallized from boiling 1,4-dioxane, dioxane solvate *rac*-DS1 forms. When dioxane solvate *rac*-DS1 suspension is boiled in methanol for 2 hours in the precipitate methanol hemisolvate *rac*-MS2 is obtained. *rac*-MS2 can also be prepared by holding any pimobendan polymorph in desiccator with methanol, however, sometimes *rac*-MS1 can also appear in this case as an impurity. After heating of *rac*-MS2 at 120 °C for more than two hours a new anhydrous polymorph *rac*-C appears. When *rac*-C is cooled to ambient temperature it immediately absorbs water and converts to hemihydrate *rac*-H3. When a suspension of pimobendan dioxane solvate *rac*-DS1 is washed with *tert*-butylmethylether and then boiled in toluene or cyclohexane and filtered, precipitate forms with very similar PXRD patterns, which contains approximately 20% of solvent (toluene or cyclohexane, respectively). The obtained form is named *rac*-G. *rac*-G can also be prepared by drying suspensions of pimobendan in other solvents (1,4-dioxane, acetone, xylene, cyclohexanol and multiple esters) at laboratory temperature in low relative humidity. Therefore, *rac*-G is a family of isostructural solvates. If *rac*-G is heated at 120 °C for approximately one day it loses almost all solvent and *rac*-G_d forms, having almost the same PXRD pattern as for the *rac*-G.

Polymorphic form *rac*-A forms in precipitate when any pimobendan polymorph or dioxane solvate *rac*-DS1 is suspended in boiling toluene or xylene (acetonitrile, nitromethane or multiple esters can also be used) for several hours.

If a hot concentrated solution of racemic pimobendan in DMF is poured into a large amount of cold water, precipitation – pimobendan hydrate *rac*-H4 forms.

1.2. Polymorphs of racemic pimobendan

Pimobendan polymorphs have notably different melting points (see Figure S1a).

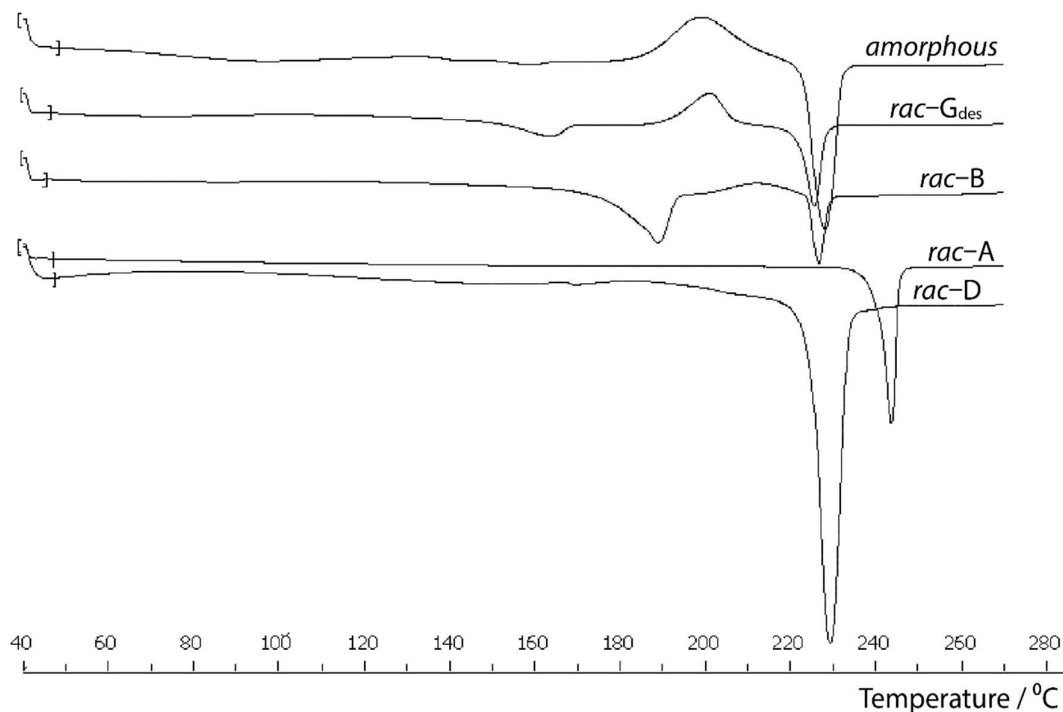


Figure S1a. DSC curves of pimobendan polymorphs (*rac*-C not shown) and amorphous phase.

After the melting polymorphs having low melting points recrystallize to one of the higher melting polymorph. In most cases *rac*-D forms as can be identified by the DSC analysis and the PXRD pattern. Recrystallization of amorphous phase is observed at 180 – 185 °C.

1.3. Hydrates of racemic pimobendan

In total four hydrates of racemic pimobendan, namely, *rac*-H1, *rac*-H2, *rac*-H3, and *rac*-H4 have been discovered. The hydrate stoichiometry was determined with Karl Fischer titration and thermogravimetry. It was determined that *rac*-H1 and *rac*-H2 are monohydrates, *rac*-H3 is a hemihydrate, whereas stoichiometry of *rac*-H4 has not been convincingly determined due to its instability, although the observed data suggests trihydrate stoichiometry. *rac*-H1, *rac*-H2, and *rac*-H3 are stable at ambient conditions while *rac*-H4 is unstable and partly transforms to monohydrate *rac*-H1 upon air-drying.

In Figure S1b TG and DSC curves of racemic pimobendan hydrates are shown.

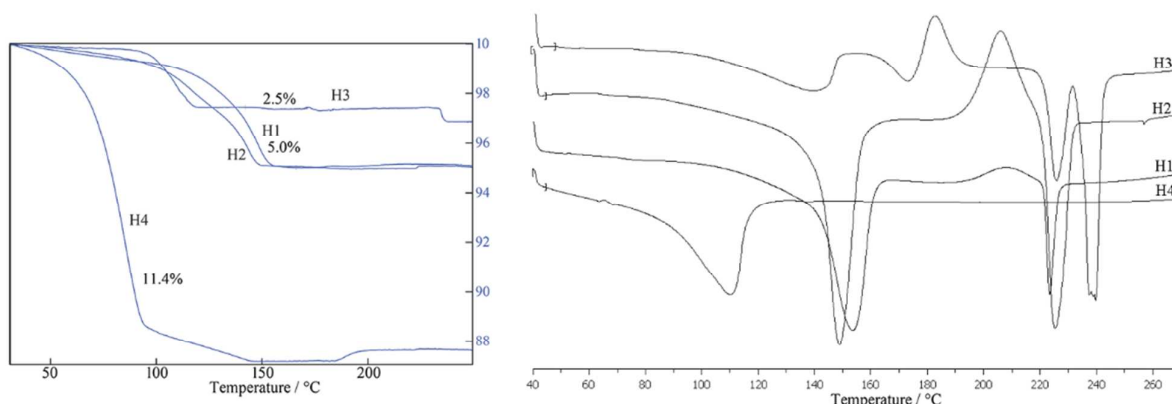


Figure S1b. TG and DSC curves of racemic pimobendan hydrates. TG curve marked as H4 is recorded for *rac*-H4 sample containing 20% of *rac*-H1.

As it can be seen from Figure S1b, *rac*-H1 and *rac*-H2 have quite similar DSC and TG curves, except the slightly different dehydration peak temperature (150-155 °C for *rac*-H1 and 145-150 °C for *rac*-H2). The dehydration of these hydrates produces an amorphous phase, which recrystallizes into polymorph *rac*-D. Dehydration peak of *rac*-H4 is below 110 °C and also its dehydration produces an amorphous phase. Temperature differences observed between DSC and TG experiments is due to different sample holder geometry and mass of the sample. *rac*-H3 dehydrates at lower temperatures than *rac*-H1 and *rac*-H2 with the dehydration peak being at 140 °C. The dehydration of *rac*-H3 always produced *rac*-C. Exposure of the obtained *rac*-C to ambient conditions leads to rapid formation of *rac*-H3.

1.4. Solvates of racemic pimobendan

TG results (Figure S1c) show that *rac*-MS1 is a methanol monosolvate, *rac*-MS2 is a methanol hemisolvate and *rac*-DS1 is a dioxane monosolvate.

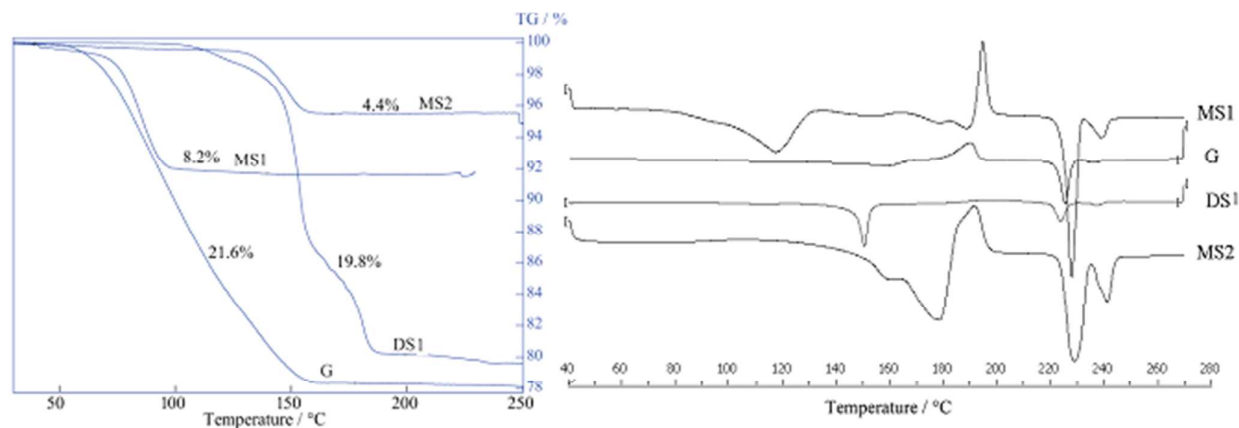


Figure S1c. TG and DSC curves of racemic pimobendan solvates.

rac-DS1 is stable in ambient conditions, while in relative humidity above 60% it transforms into monohydrate *rac*-H1. *rac*-MS1 desolvates at lower temperature if compared to the *rac*-DS1 and *rac*-MS2. This is in agreement with the fact that in ambient conditions *rac*-MS1 decomposes after one day, while *rac*-MS2 slowly transforms into *rac*-H3 and in ambient conditions complete transformation takes more than three months.

Furthermore, kinetics of *rac*-MS2 to *rac*-C solid state transformation was studied, revealing that it is a direct transformation corresponding to geometrical contraction kinetic model R3 (see Figure S1d).

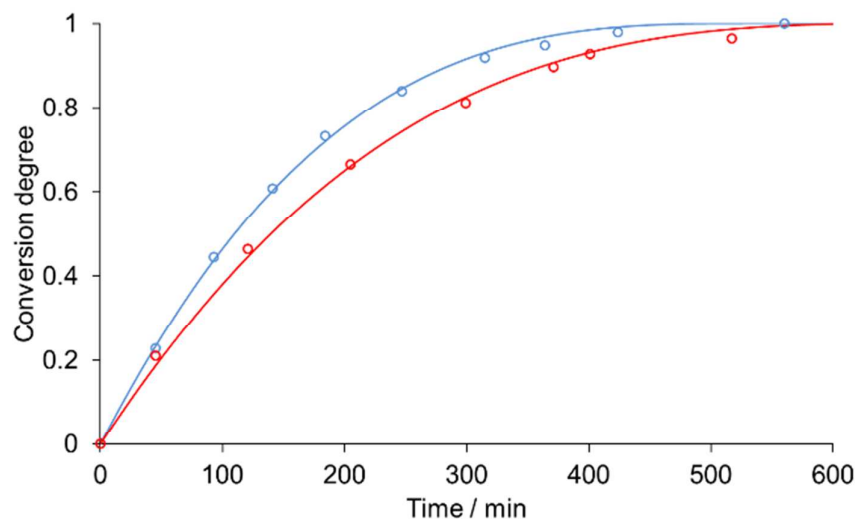


Figure S1d. Conversion degree of the transformation *rac*-MS2 to *rac*-C versus time at varying relative humidity (3.5% – red and 5.0% – blue). Data points from quantitative PXRD analysis depicted as open circles, theoretical curves of kinetic model R3 depicted as solid lines.

Desolvation of *rac*-G (prepared from toluene) is not detectable by the DSC, while from the TG analysis it is determined that it desolvates in a broad temperature range up to 150 °C. Both of these facts lead to conclusion that *rac*-G is a nonstoichiometric solvate. Furthermore, several isostructural solvates were discovered. PXRD patterns and TG curves of crystalline form *rac*-G prepared from various solvents are shown in Figure S1e and S1f.

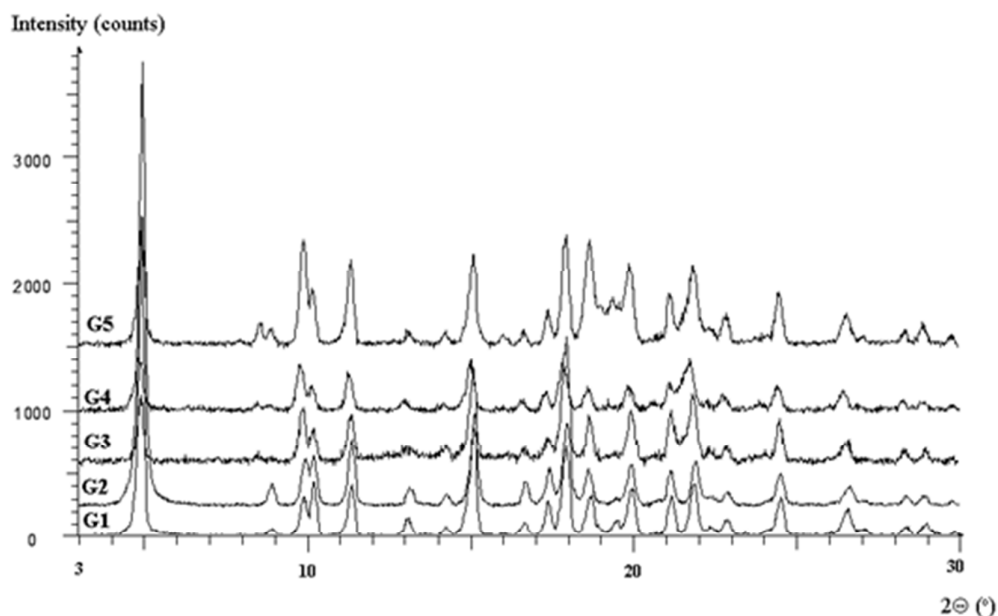


Figure S1e. PXRD patterns of racemic pimobendan solvates *rac*-G (1 – toluene, 2 – cyclohexane, 3 – 1,4-dioxane, 4 – ethyl acetate, 5 – acetone).

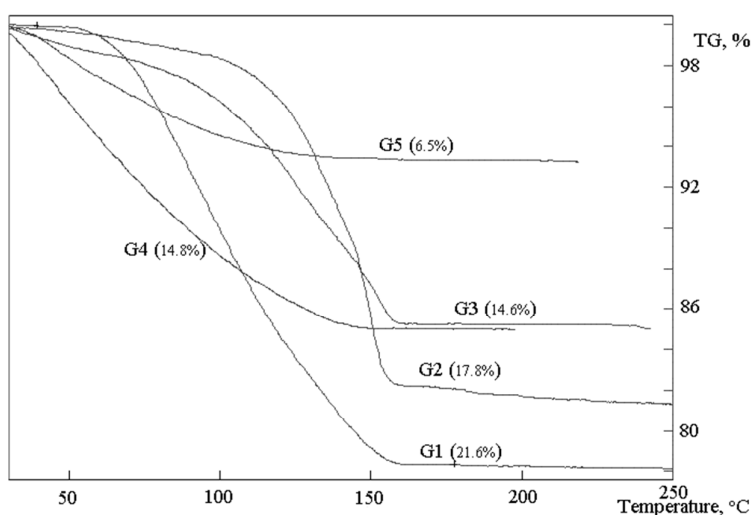


Figure S1f. TG curves of racemic pimobendan solvates *rac*-G (1 – toluene, 2 – cyclohexane, 3 – 1,4-dioxane, 4 – ethyl acetate, 5 – acetone).

In the Figures above data for *rac*-G crystallized from toluene (G1), cyclohexane (G2), 1,4-dioxane (G3), ethyl acetate (G4) and acetone (G5) are shown, but there are other solvents from which *rac*-G can be obtained including various esters, xylene and cyclohexanol. As it can be seen from Figure S1e, PXRD patterns of solvates *rac*-G are almost identical in terms of the diffraction peak positions and intensities. However, the intensity of peak at 4.9° appears to be solvent as well as solvent content dependent. Indexation of the PXRD patterns revealed that solvates *rac*-G crystallize in the monoclinic crystal system. In Table S1 values of lattice parameters and phase composition of the obtained isostructural solvates are given.

Table S1. Phase composition and lattice parameters of isostructural nonstoichiometric solvates *rac*-G

Solvent	Mass loss during desolvation / %	Stoichiometry	Lattice parameters			
			$a / \text{\AA}$	$b / \text{\AA}$	$c / \text{\AA}$	$\beta / ^\circ$
toluene	21.6	1.0	10.437	17.898	10.804	108.588
cyclohexane	17.8	0.9	10.448	17.763	10.835	108.785
1,4-dioxane	14.6	0.7	10.429	17.902	10.904	108.796
ethyl acetate	14.8	0.7	10.465	17.889	10.823	108.609
acetone	6.5	0.4	10.428	17.925	10.845	108.517
xylene	18.8	0.8	10.434	17.906	10.817	108.521
cyclohexanol	17.4	0.8	10.507	17.979	10.906	108.589
butyl acetate	19.8	0.8	10.496	17.949	10.848	108.569
Ethyl formate	10.5	0.6	10.444	17.939	10.899	108.585
methyl acetate	11.2	0.6	10.412	17.858	10.851	108.611
propyl acetate	12.3	0.5	10.479	17.961	10.904	108.596
propyl formate	17.0	0.8	10.439	17.859	10.906	108.622
average			10.45	17.90	10.86	108.62
G _d			10.376	17.820	10.836	108.709

2. DSC and PXRD data used to establish the melt phase diagram of pimobendan enantiomers

2.1. Solid solutions α and ζ

The DSC curves for samples obtained crystallizing different enantiomeric composition samples of pimobendan from acetonitrile / ethyl acetate solutions are shown in Figure S2.

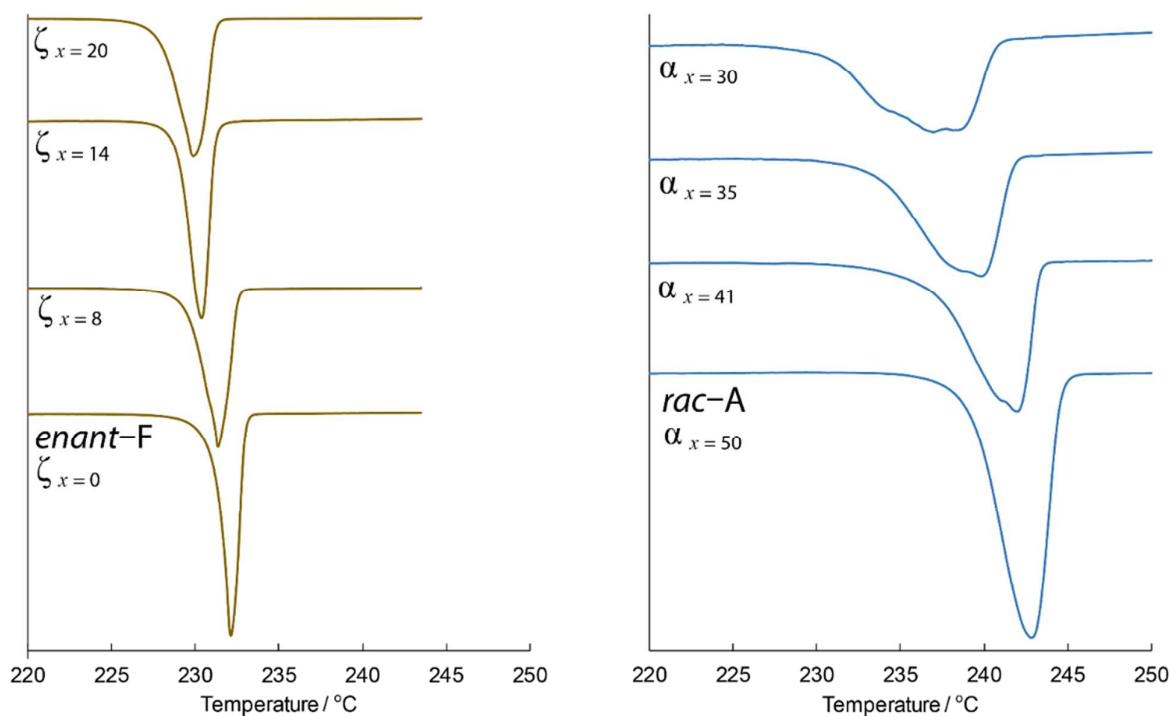


Figure S2. DSC curves of different composition samples of pimobendan crystallized from acetonitrile / ethyl acetate solutions (exo ^).

PXRD patterns are given in Figure S3.

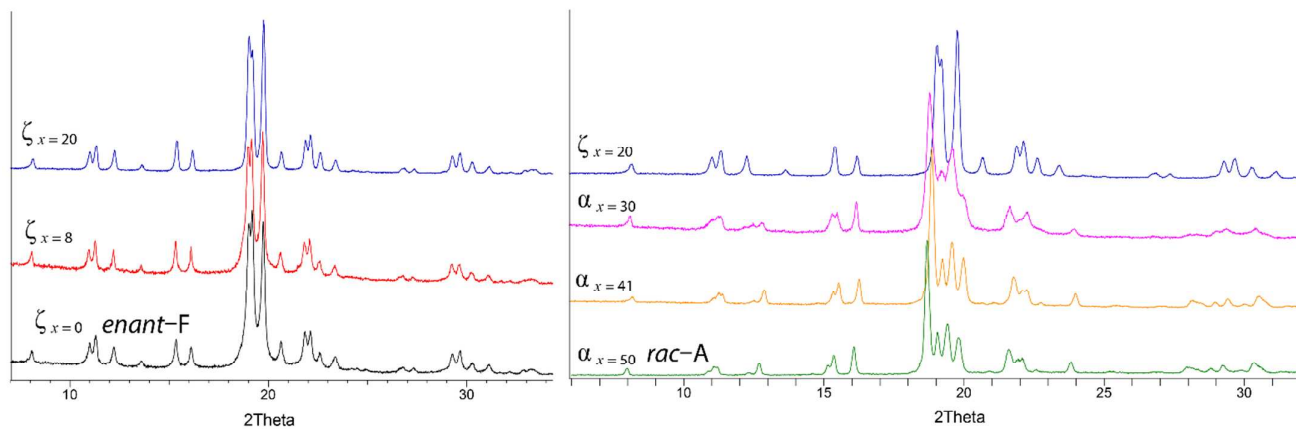


Figure S3. PXRD patterns of different composition samples of pimobendan crystallized from acetonitrile / ethyl acetate solutions.

PXRD data show that crystallizing different enantiomeric composition samples of pimobendan and after complete evaporation of the solvent mixture phases are obtained with diffraction patterns being very similar to either pimobendan polymorphs *enant*-F or *rac*-A. It indicates that single phase are obtained corresponding to solid solutions of enantiomers. DSC data complement PXRD data showing that there is no eutectic melting present.

2.2. Solid solutions δ and γ

Solid solutions δ and γ were obtained desolvating respective solvated forms. DSC curves and PXRD patterns of solid solution δ are given in Figure S4 and S5.

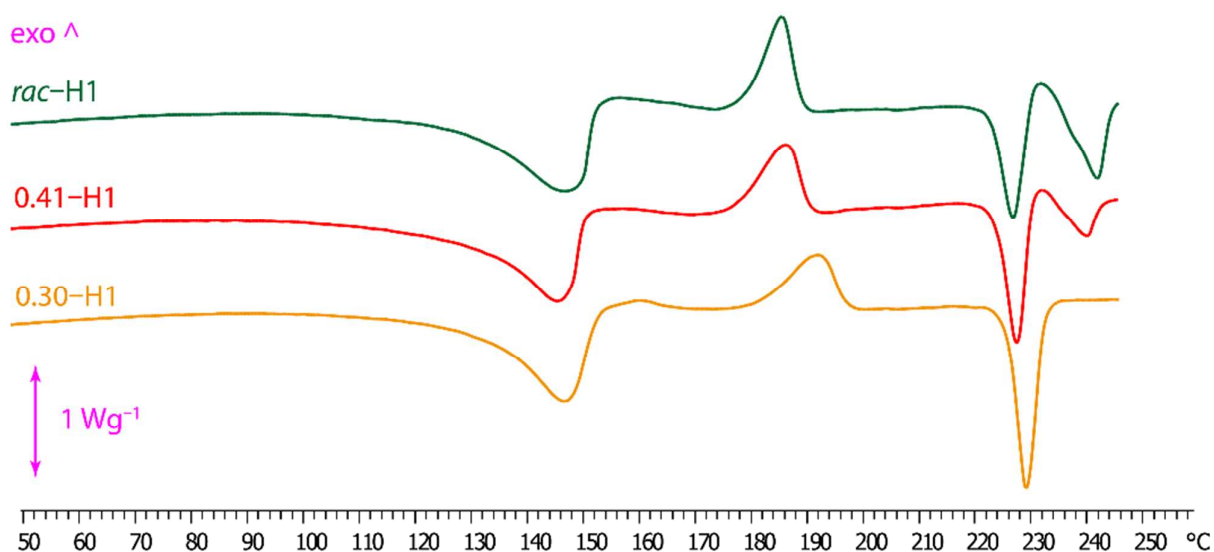


Figure S4. DSC curves of different composition samples of pimobendan monohydrate H1 heated at a rate of $5 \text{ K} \cdot \text{min}^{-1}$ in open pans.

The first endothermic peak corresponds to the dehydration event, after that recrystallization is observed. The following endothermic peak corresponds to melting of solid solution δ . In case of racemic and 0.41 composition subsequent recrystallization occurs giving solid solution α , which immediately melts. Absence of solid solution α formation for 0.30 enantiomeric composition sample can be explained by the fact that it is not so stable anymore. The onset of the melting peak of $\alpha_{X=0.30}$ overlaps with the melting of $\delta_{X=0.30}$.

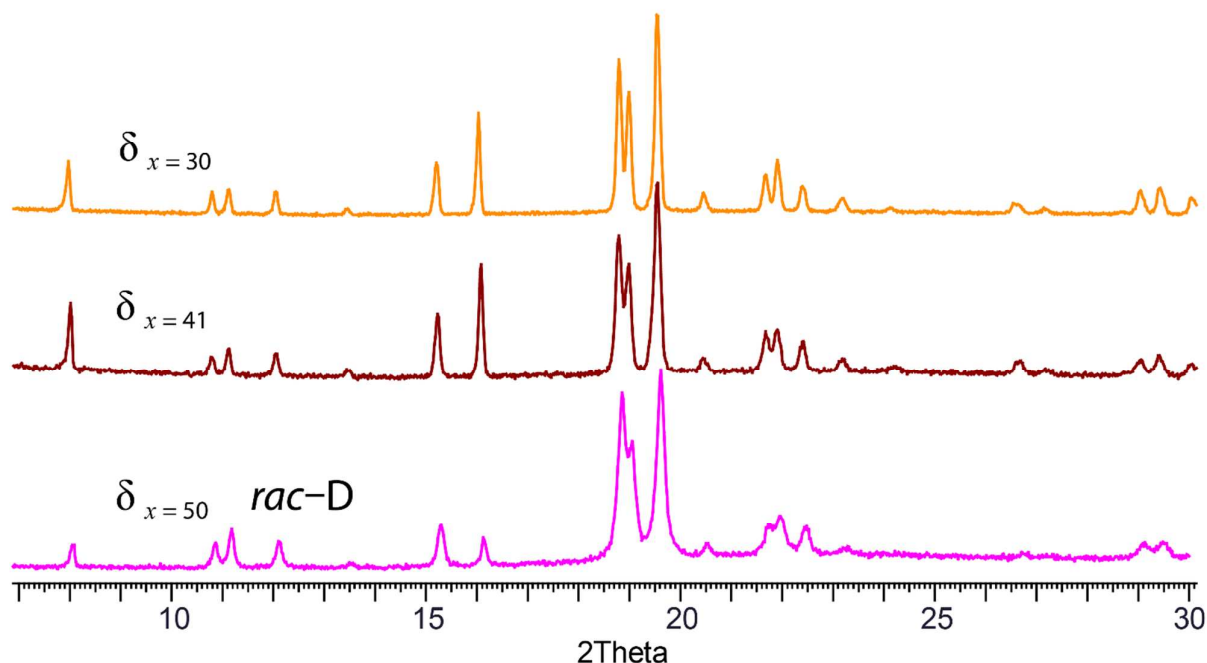


Figure S5. PXRD patterns of pimobendan solid solution δ (form D).

Solid solution γ is obtained by desolvating pimobendan methanol solvate MS2 (DSC data given in Figure S6). In case MS2 is used as a starting material for the analysis the first endothermic peak corresponds to the desolvation event, TG curves show $\sim 4.5\%$ weight loss corresponding to hemimethanolate. After desolvation form C melts which is observed as a broad endothermic event. When form C (pre-desolvated MS2) is used as a starting material for DSC analysis a broad endothermic peak of C form melting is observed, which overlaps with an exothermic recrystallization peak. Furthermore, apparently at the recrystallization form D is obtained as the following endothermic peak corresponds to the melting of form D (solid solution δ). Due to overlap it is not possible to surely assess the onset based on the DSC curves where form C is used as a starting material. For MS2 samples, however, the melting event partly overlaps with the desolvation event also complicating the determination of the onset. For the reasons mentioned peak maximum has been used from MS2 experiments to depict in the phase diagram. It must be added that no better data at different heating rates or compositions could have been obtained. Preparation of MS2 often leads to mixtures of both methanol solvates (MS2 and MS1). For this kind of study where different enantiomeric composition samples are used to construct a phase diagram phase purity is crucial for right interpretation of the DSC data.

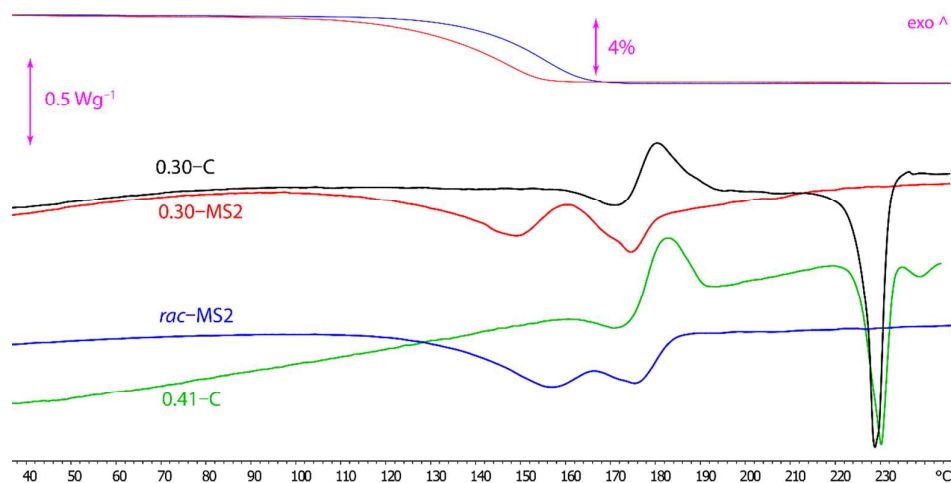


Figure S6. DSC curves of different composition samples of pimobendan methanol solvate MS2 and form C heated at a rate of 5 K·min⁻¹ in open pans. TG curves given with thinner lines.

PXRD patterns of different enantiomeric composition forms C (solid solution γ) are given in Figure S7.

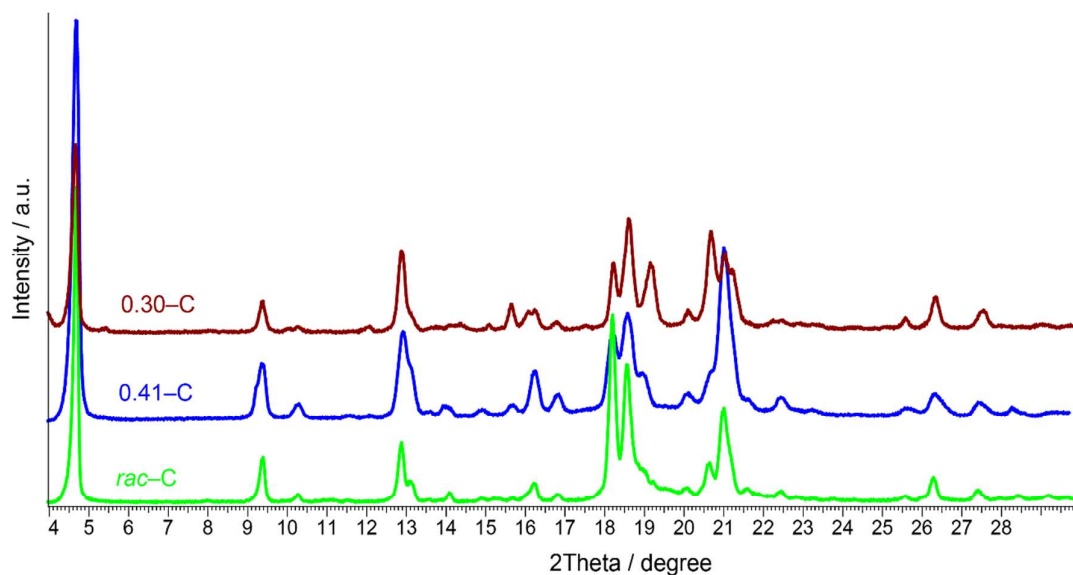


Figure S7. PXRD patterns of pimobendan solid solution γ (form C).

Observed changes of peak positions and intensities in the PXRD patterns are due to change of unit cell parameters and atomic positions.

3. Evidence of solvated solid solutions of pimobendan enantiomer phases

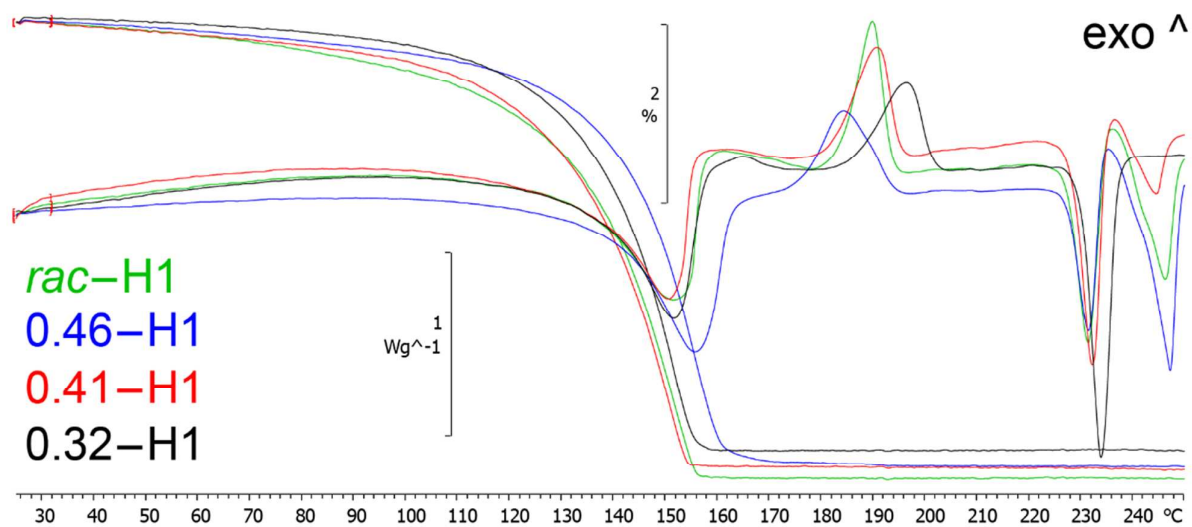


Figure S8. TG/DSC curves of pimobendan monohydrate *rac*-H1 solid solutions.

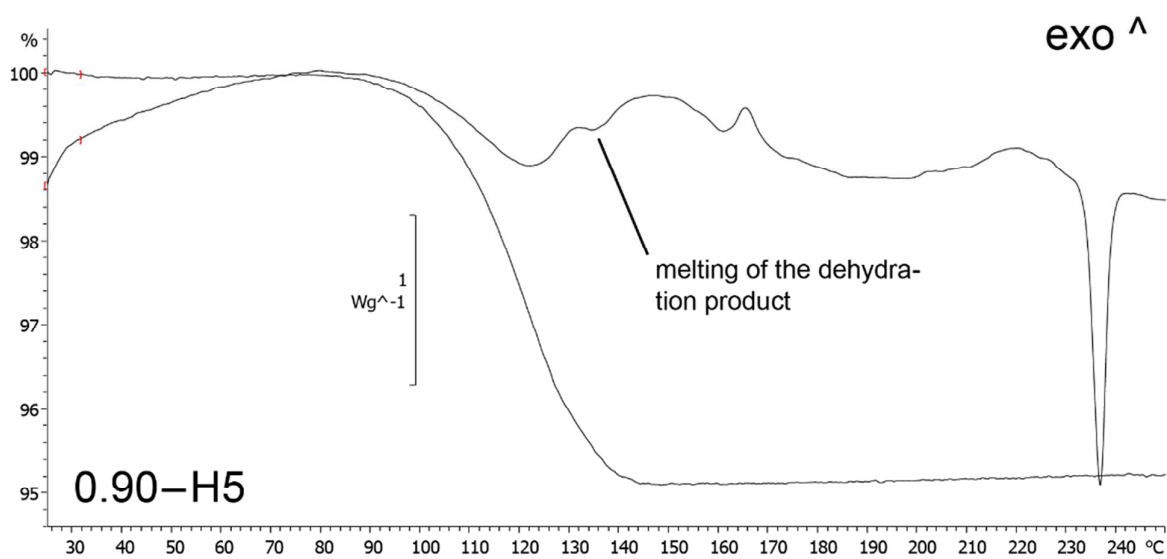


Figure S9. TG/DSC curves of pimobendan monohydrate 0.90-H5 (0.10-H5) solid solution.

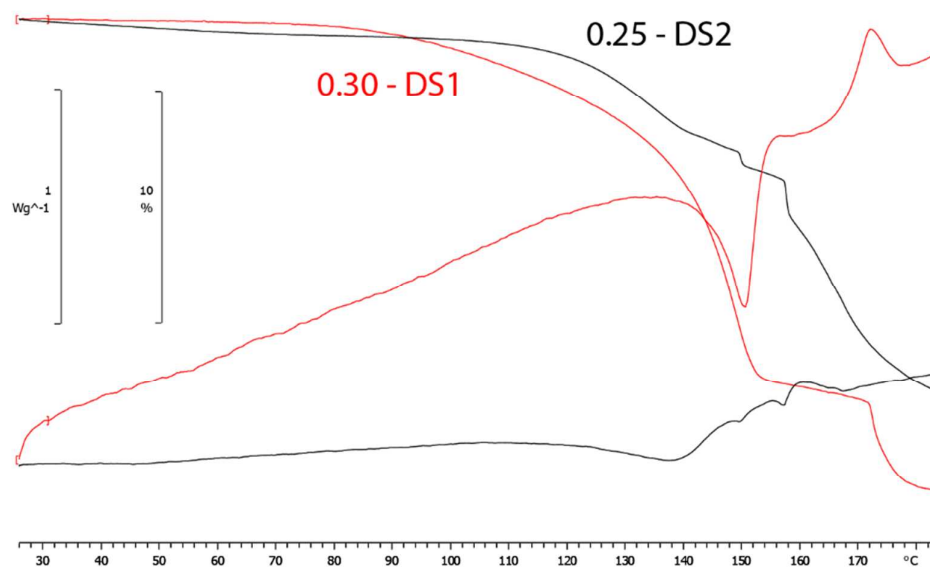


Figure S10. TG/DSC curves of pimobendan dioxane monosolvates 0.25-DS2 and 0.30-DS1 solid solutions.

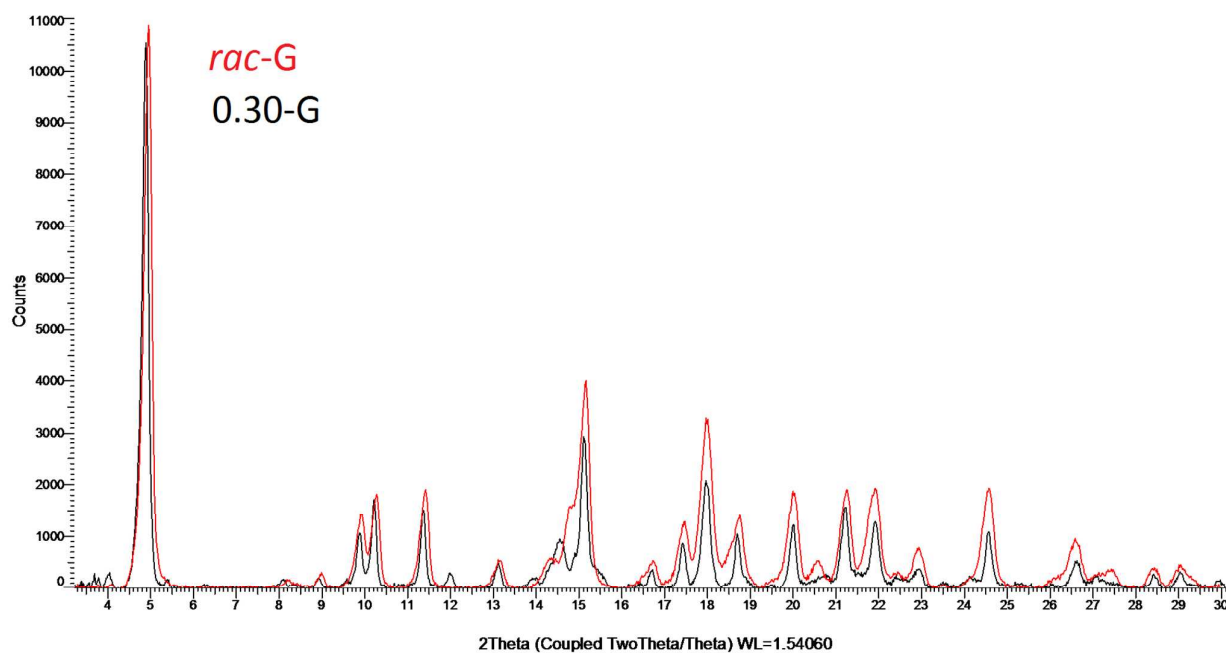


Figure S11. PXRD patterns of pimobendan toluene solvate $G_{toluene}$ solid solutions.

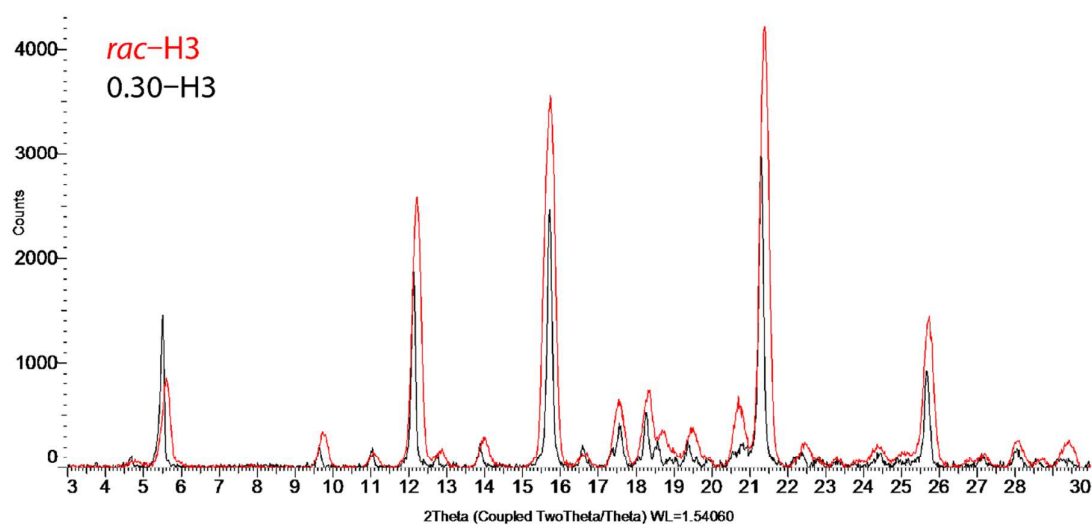


Figure S12. PXRD patterns of pimobendan hemihydrate H3 solid solutions.

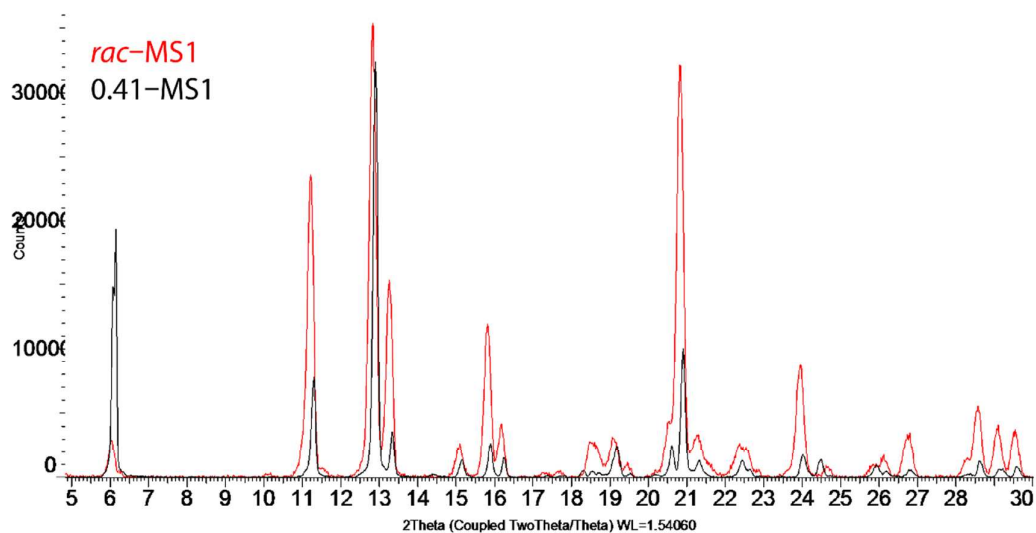


Figure S13. PXRD patterns of pimobendan methanol monosolvate MS1 solid solutions.

4. Experimental and calculated PXRD patterns of *enant*-F

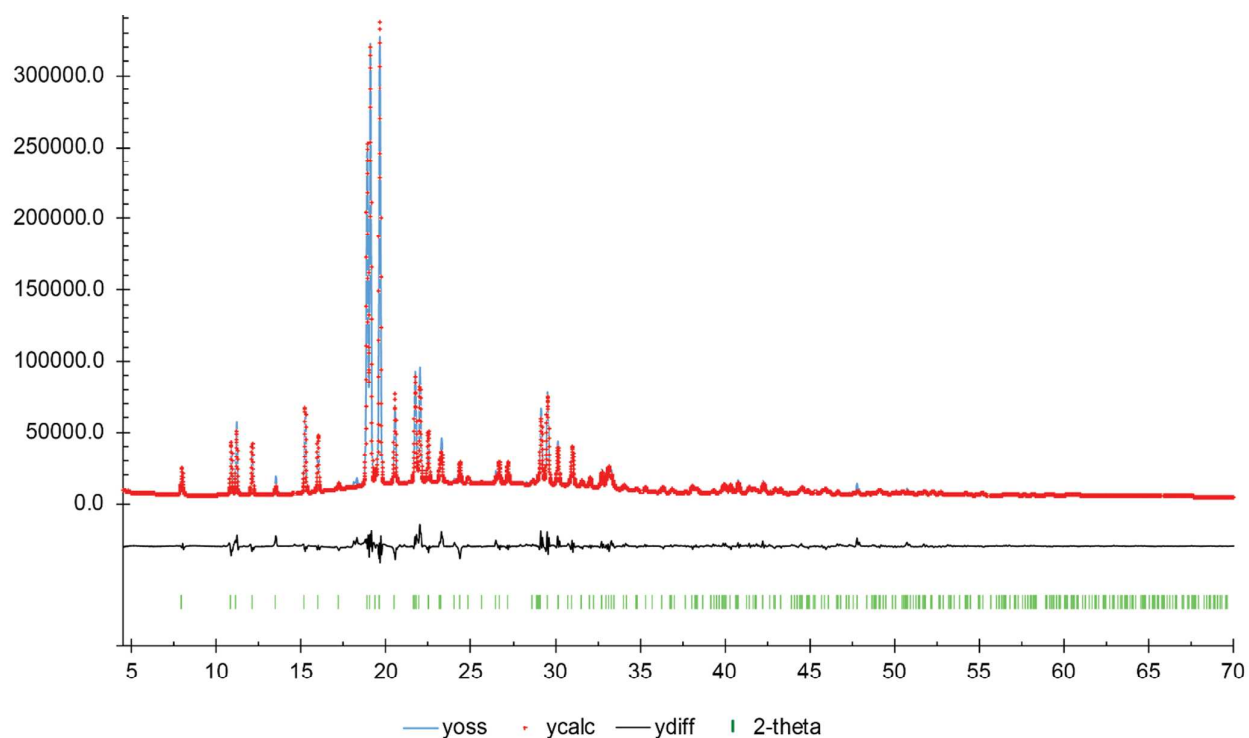


Figure S14. Experimental and calculated PXRD patterns of *enant*-F.

There are a few minor PXRD peaks (see e.g. two peaks at around 18-19 2θ in Figure S8 and S9) not present in the calculated pattern arising from a minor W- $L\alpha_1$ radiation presence in the primary Cu- $K\alpha_1$ radiation (due to deposition of tungsten from the X-ray tube cathode onto its copper anode).

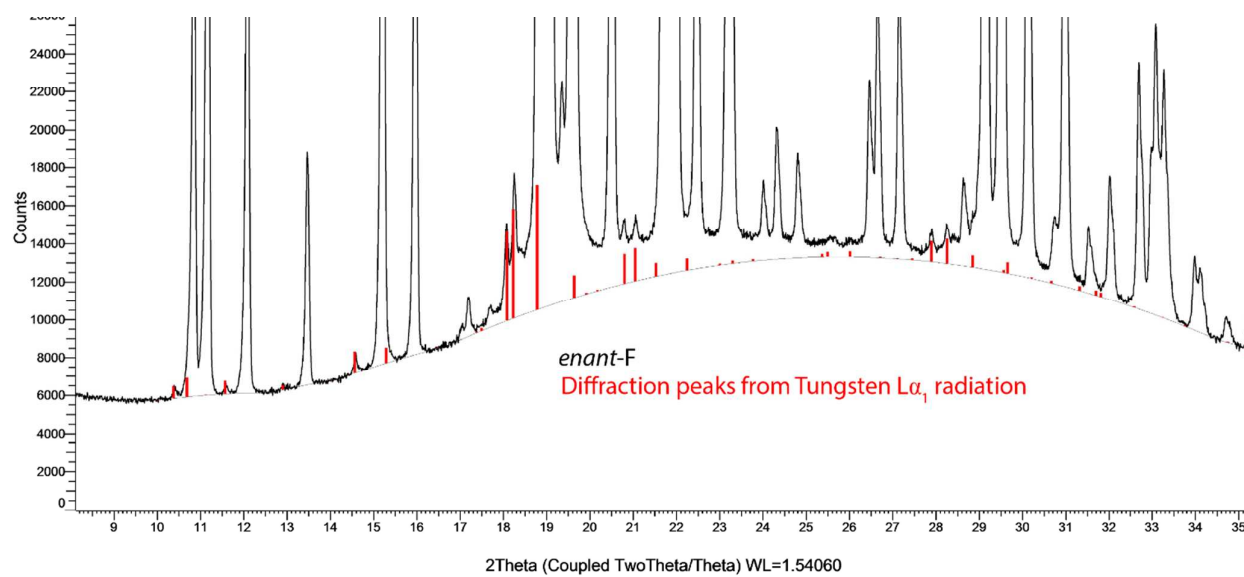


Figure S15. PXRD pattern of *enant-F* showing peaks arising from W-L α_1 radiation.